Ab initio depolarization in self-assembled molecular monolayers: Beyond conventional density-functional theory

M. Piacenza, S. D'Agostino, E. Fabiano, and F. Della Sala
National Nanotechnology Laboratory of INFM-CNR, Distretto Tecnologico ISUFI, Via per Arnesano, I-73100 Lecce, Italy
(Received 25 August 2009; published 2 October 2009)

We present an efficient *ab initio* atomic-orbital-based embedding scheme, which allows to describe depolarization effects in self-assembled organic monolayers (SAMs). The method includes periodic-boundary conditions, all multipole moments and local-field effects. Results for substituted oligophenyl SAM, in combination with conventional, hybrid and orbital-dependent density-functional theory (DFT) as well as coupled-cluster (CC) approach, are reported. We find that the accuracy of conventional DFT relies on error cancellation between the concurrent overestimation of dipole and polarizability, but it can yield quantitatively and sometimes even qualitatively wrong results. Hybrid and orbital-dependent functionals strongly improve the overall description and closely reproduce CC results.

DOI: 10.1103/PhysRevB.80.153101 PACS number(s): 34.35.+a, 31.15.E−, 77.22.Ej

Organic-metal interfaces play a key role in different nanoscience research areas, such as molecular electronics[1] and organic (opto)electronics.[2] When an organic molecule is chemi- or physiadsorbed on a metal surface, its workfunction changes due to the formation of an interfacial dipole.[2] In organic (opto)electronic devices self-assembled monolayers (SAMs) of organic molecules with tailored dipole moment can be used to align the metal workfunction to the molecular-orbital energy of the organic film to enhance the current transport.[3,4]

The work-function shift ($\Delta\Phi$) can be computed using the Helmholtz equation $\Delta\Phi(n)=-4\pi n\mu_z(n)$, where n is the number of molecules per unit area and $\mu_z(n)$ the component of the molecular interface dipole perpendicular to the surface.[2,5] $\mu_z(n)$ can be further divided into two contributions $\mu_z(n)=\mu_z^S(n)+\mu_z^{chem}(n)$, where μ_z^S is the dipole moment of the isolated SAM and μ_z^{chem} is the bond dipole, related to the electronic charge reorganization at the interface.[6,7] In SAM of polar organic molecules μ_z^S is the largest component and mainly determines the work-function shift.[6–8]

In first approximation μ^S can be calculated considering the monolayer as a two-dimensional lattice of point dipoles. Within this approximation, μ^S is given by the Topping formula[9,10] (generalized here for anisotropic systems)

$$\underline{\mu}^S(n) = \underline{\mu}^0 + \underline{\underline{\alpha}}\underline{E}_d(n) = [\underline{\underline{I}} + n^{3/2}\underline{\underline{\alpha}}\underline{\underline{Q}}]^{-1}\underline{\mu}^0, \qquad (1)$$

where $\underline{\mu}^0$ is the dipole moment of an isolated molecule, $\underline{E}_d(n)=-n^{3/2}\underline{\underline{Q}}\underline{\mu}^S$ is the depolarizing electric field, $\underline{\underline{\alpha}}$ is the molecular polarizability tensor and $\underline{\underline{Q}}$ is a diagonal matrix which depends only on the lattice type.[9,10] The Topping model is not expected to work in a closely packed monolayer due to the point-dipole approximation. Improvement over the Topping formula is obtained by explicitly considering the molecular electronic structure. This is achieved, e.g., in the semiempirical quantum chemistry (SEQC) methods by simulating a portion of the SAM using a finite-cluster approach[11] or by computing atom-atom polarizabilities.[12] The SEQC method can include local-field effects, but suffers from the semiempirical parametrization and/or from the finite size of the cluster because of the poor convergence of electronic properties with the system size. To avoid finite-size effects periodic-boundary conditions (PBCs) must be used. A popular approach is first-principles plane-wave density-functional theory (PW-DFT) within the supercell and dipole-correction scheme.[13] The PW-DFT approach offers in principle an exact description of the depolarization effect, but it cannot easily treat the low-coverage regime and more importantly is generally applied using conventional DFT functional, i.e., the local-density approximation (LDA) or the generalized-gradient approximation (GGA). This limits the accuracy of PW-DFT results, as LDA/GGA functionals face severe drawbacks in the calculation of dipole moments[14] and polarizabilities[15] of extended conjugated systems. The use of hybrid,[16] orbital-dependent functionals[17] and coupled-cluster methods which better describe the electronic properties of organic molecules would then be desirable. Despite recent progress,[18,19] their applicability is still hampered by the high computational costs within PBC.

In this work we present an efficient method to describe the SAM depolarization, namely the self-consistent periodic-image-charges embedding (SPICE) approach. The SPICE method is based on an atomic-orbital (AO) electrostatic embedding scheme, and allows to compute the SAM depolarization for any coverage, using PBC and any AO-based electronic-structure method (e.g., hybrid or orbital-dependent functionals, correlated wave-function methods). In the SPICE approach the SAM dipole is evaluated from the electronic density ρ of a single molecule embedded in the two-dimensional monolayer. The density of a molecule in the SAM is related to the density of the isolated molecule $\rho^0(\mathbf{r})$ by the formula

$$\rho(1) = \rho^0(1) + \chi(1,2)V_{ext}(2) \qquad (2)$$

where $\chi(1,2)=d\rho(1)/dV_{ext}(2)$ is the nonlocal charge-density susceptibility (reducible polarizability) and V_{ext} is the perturbing potential due to the interaction with all other molecules in the SAM. In this work we restrict V_{ext} to be the Coulomb potential, which is dominant at low coverages. To treat very high coverages Eq. (2) must be generalized to

include exchange-correlation contributions. Thus, the perturbing potential is

$$V_{ext}(2) = \hat{\mathcal{T}}(2)v(2-3)(\rho(3) - \rho^N(3)), \tag{3}$$

where $v(2-3)=1/\|\mathbf{r}_2-\mathbf{r}_3\|$ is the bare coulomb interaction, $\hat{\mathcal{T}}$ is the periodic image sum operator (creating periodic images and summing over all the unit cells) and $\rho^N(\mathbf{r})=\Sigma_{I=1}^N Z_I\delta(\mathbf{r}'-\mathbf{R}_I)$ is the nuclear charge. Substituting Eq. (3) into Eq. (2) and defining the total charge $q=\rho-\rho^N$, we have

$$q(1) = q^0(1) + \chi(1,2)\hat{\mathcal{T}}(2)v(2-3)q(3), \tag{4}$$

which describes the change in the charge density due to the electrostatic interaction between the molecules in the SAM. The corresponding relation for the dipoles is readily obtained by multiplication by $\mathbf{r}_1$, using the definition $\chi(1,2)=\underline{\nabla}_{(1)}\underline{\nabla}_{(2)}:\underline{\underline{\alpha}}(1,2)$,[20] where $\underline{\underline{\alpha}}(1,2)$ is the nonlocal polarizability, and integrating (by parts in the right-hand side). It reads as

$$\underline{\mu}^S = \underline{\mu}^0 + \int d1\,\underline{\underline{\alpha}}(1,2)\hat{\mathcal{T}}(2)\underline{\nabla}_{(2)}v(2-3)q(3). \tag{5}$$

Equation (5) includes all multipolar contributions and local-field effects and it is reduced to the Topping formula (1) by introducing (i) the point-dipole approximation leading to $E_d(2)=\hat{\mathcal{T}}(2)\underline{\underline{T}}(2)\underline{\mu}$, with $\underline{\underline{T}}$ the second-rank dipole tensor,[20] and (ii) averaging over the unit cell to obtain the averaged polarizability $\underline{\underline{\alpha}}$ in Eq. (1).

Equation (4) must be solved self-consistently, but a direct solution is in general impossible because no explicit formula for the susceptibility χ is available and approximations are usually employed.[12] In the SPICE method this difficulty is overcame by splitting the self-consistent procedure into two steps: (i) the periodic perturbing potential in Eq. (3) is computed, for a given a charge distribution q; (ii) the charge distribution is computed by solving the Schrödinger equation for the molecular system in the external potential V_{ext}. The two steps are repeated in a double self-consistent loop until convergence is achieved. In step (ii) the new charge distribution can be computed by any electronic-structure method without explicit computation of χ.

The SPICE method has been implemented in the TURBOMOLE (Ref. 21) program package. To enhance the computational efficiency in our implementation the perturbing periodic potential was evaluated by fitting the electrostatic potential of a single molecule with point charges (Mulliken charges) and using the periodic charge embedding (PCEMB) (Ref. 22) approach to obtain the full periodic potential. The quality of the point-charges fit had to be carefully verified to avoid inaccuracies in the embedding potential. The external self-consistent loop was considered converged when the induced dipole moment converged to 10^{-3} a.u. (which always occurred within ten cycles).[23] DFT calculations were performed using the Perdew-Burke-Ernzerhof (PBE) (Ref. 24) functional, the hybrid PBE0 (Ref. 25) and the orbital-dependent localized Hartree-Fock (LHF) (Ref. 26) method with a LYP correlation functional.[27] We also considered the Hartree-Fock (HF) and the approximate coupled-cluster single double method (CC2).[28,29] In the latter relaxed densities were employed. The TZVP basis set[30] and spin-polarized wave functions were used in all calculations.

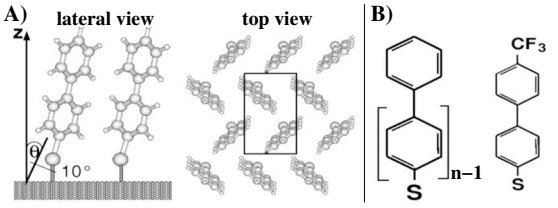

FIG. 1. Structure of (A) mercapto-biphenyl SAM; (B) investigated molecules ($n=1-4$).

In order to assess the method, we applied it to mercapto-biphenyl [see Fig. 1(a)], which has been subject of recent detailed studies,[7,31] and compared the results to the ones obtained from plane-wave pseudopotential (PWPP) calculations. We optimized the molecular geometry for a dense coverage on the Au(111) surface, using the PWSCF (Ref. 32) program with the PW91 functional and a kinetic-energy cutoff of 35 Ryd. The supercell consisted of five gold layers, 40 Å vacuum and two molecules arranged in a herringbone pattern on a $\sqrt{3}\times 3$ surface unit cell with an angle from the surface normal of about 10° [see Fig. 1(a)]. This structure was used in all subsequent electronic-structure calculations. Starting from the full coverage regime we obtained lower coverages following the procedure of Ref. 33. The SAM dipole was computed for all coverages using the PBE functional and the dipole-correction scheme.[13]

Figure 2(a) shows the comparison between PBE results obtained with the SPICE approach, PWPP calculations and the Topping model. In the latter the dipole vector and polarizability tensors of an isolated molecule computed at the PBE level were used. At vanishing surface molecular density ($n=0$) all methods yield close results (the SPICE and Topping model coincide by construction). We found that the remaining small differences between SPICE and PWPP are related to different details of the electronic-structure calculations (e.g., all-electron vs pseudopotential). At higher coverages the Topping formula significantly underestimates the dipole moment because of the neglect of high multipole moments and local-field effects. The SPICE method instead yields results always in perfect agreement with the PWPP calculations. Notably, the SPICE approach performs well also at high coverages, despite nonzero wave-function overlap.

After assessing the accuracy of the model we applied it in combination with different computational approaches (PBE0, LHF-LYP, HF, and CC2) to investigate the role of the electronic-structure description. Figures 2(b) and 2(c) report the computed SAM dipole and the work-function shift. Figure 2(b) shows that the PBE functional overestimates (with respect to CC2, our reference) the dipole at zero coverage by about 30%. At higher coverages the depolarization effect reduces the dipole more significantly for PBE than for the other methods. This behavior is related to the too high PBE polarizability (α_{zz} is 359, 325, 320, 285, and 218 a.u. for PBE, CC2, PBE0, LHF-LYP and HF respectively). The overestimation (underestimation) of the LDA/GGA (HF) polariz-

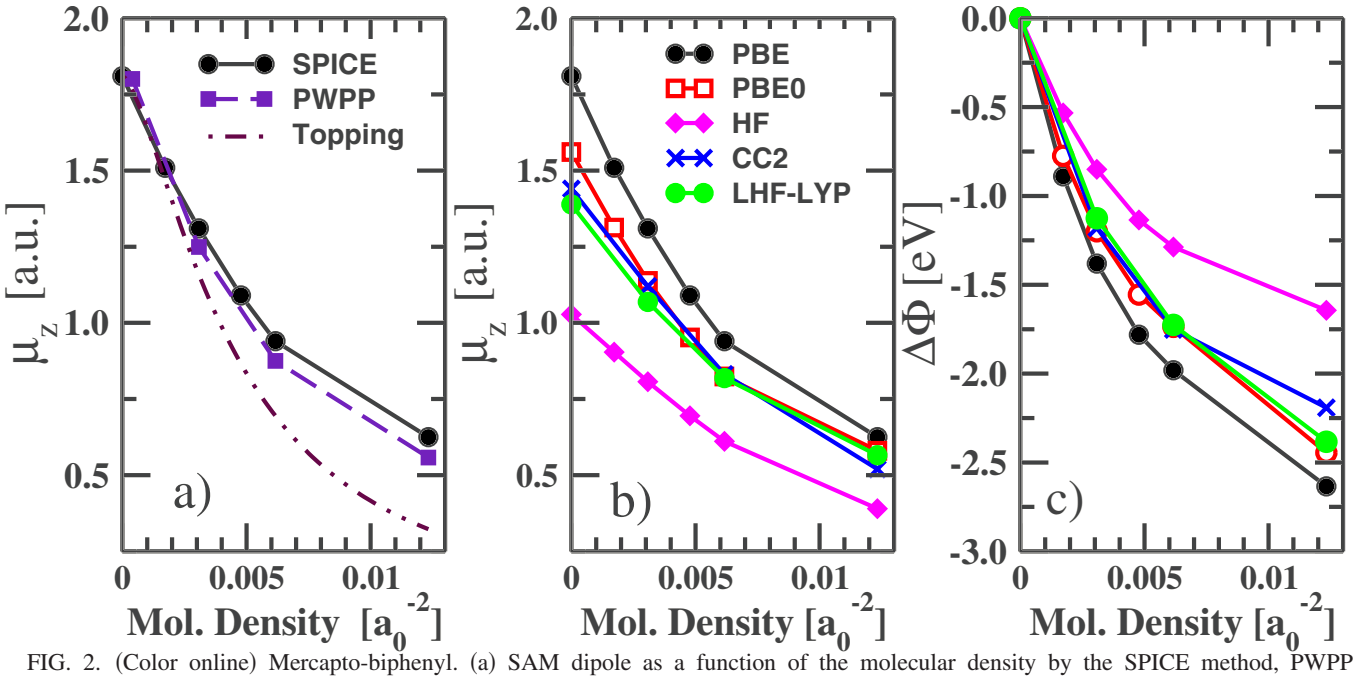

FIG. 2. (Color online) Mercapto-biphenyl. (a) SAM dipole as a function of the molecular density by the SPICE method, PWPP calculations and the Topping model (PBE functional). (b) SAM dipole and (c) work-function shift as a function of the molecular density, by the SPICE method using different electronic-structure approaches.

ability in oligomers is well documented,[15] and results close to the CC2 reference are only obtained from hybrid and effective exact-exchange methods. The simultaneous overestimation by PBE of the dipole and polarizability leads to a partial error cancellation at high coverages. Nevertheless, at the highest coverage an overestimation of $|\Delta\Phi|$ by about 0.45 eV is found [see Fig. 2(c)] which is non-negligible to engineer organic-metal interfaces for (opto)electronic applications. Opposite results are obtained for the HF method, due to the neglect of electron correlation. Finally, PBE0 and the LHF-LYP method exactly reproduce the CC2 results, but for the highest coverage.

In order to clarify how the differently computed dipoles and polarizabilities influence $\Delta\Phi$, we investigated the model systems shown in Fig. 1(b), with (I) increasing number of oligomers and (II) electron accepting substituent. In the first case we investigated oligophenylthiolate model systems of chain length $n=1-4$. Molecular geometries were obtained from B3LYP/TZVP optimizations[16,27] using a C_{2v} symmetry constraint. The molecular orientation was chosen in perfectly perpendicular alignment with respect to an ideal surface in order to restrict the contribution of the molecular dipole moment to μ_z. The cell parameters were varied from 30 to 10 bohr, to obtain surface molecular densities similar to those employed in Fig. 2. Figures 3(a) and 3(b) report the molecular dipoles for PBE and PBE0 at different chain lengths; the CC2 results (not reported) are close to PBE0. The PBE overestimation of the dipole increases with the oligomer size due to the delocalization error of conventional DFT methods.[14,15] However, also the polarizability increases with the chain length (e.g., for $n=4$ we obtain 1080 and 842 a.u. for PBE and PBE0, respectively). Thus, increasing the surface molecular density the total dipole decays faster in PBE than in PBE0, yielding for high coverages similar results with all methods and all chain lengths. The good performance of the PBE functional at high coverage is therefore fortuitous and only relies on an error cancellation effect. Poor results are obtained instead at low coverage.

Figure 3(c) shows the modification of the charge density [$\Delta\rho=\rho-\rho^0$, see Eq. (2)] due to the packing effects. Increasing the molecular density a remarkable depletion of charge at the sulfur with consequent accumulation in the molecular backbone is observed. This causes the formation of an induced dipole with opposite direction with respect to that of the isolated molecule. The effect is larger for PBE than for PBE0. The high oscillating behavior of the density is typical

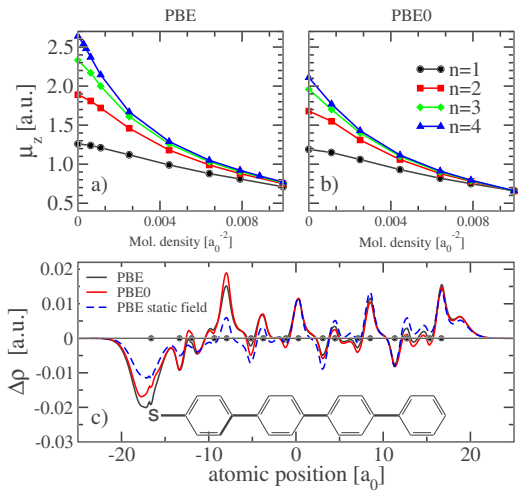

FIG. 3. (Color online) Model oligomers $n[1-4]$. Upper Panels: SAM dipole moments for PBE (a) and PBE0 (b) as a function of the molecular density. Lower panel (c): difference of the electronic density (averaged over the plane perpendicular to the long axis of the molecule) between the highest coverage and the isolated molecule, for PBE and PBE0. The electronic density induced by an uniform field is also shown for PBE.

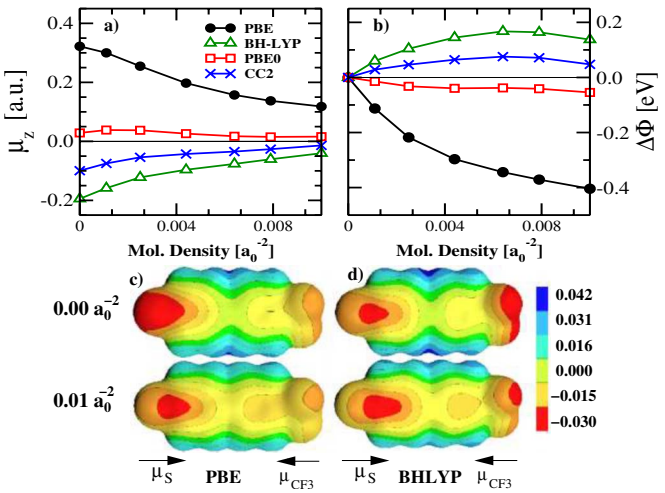

FIG. 4. (Color online) CF_3 substituted biphenyl. Upper panel. (a) SAM dipole moment and (b) work-function shift as a function of the coverage. Lower panel. Electrostatic potential for different coverages for (c) PBE and (d) BHLYP.

for oligomers.[33] As the local electric field is larger near the sulfur atom (where the dipole is mainly localized), the SPICE model correctly predicts a larger $\delta\rho$ than using an unifrom electric field [see dashed line in Fig. 3(c)].

Error cancellation cannot occur when dipole or polarizability are badly described, e.g., in systems with a strong acceptor group. Such a situation is depicted in Figs. 4(a) and 4(b) where the dipole and work-function shift of the trifluoromethyl substituted biphenyl are reported. At zero coverage, the absolute value of the PBE dipole is significantly smaller than the ones presented in Figs. 2 and 3 because the CF_3 substituent induces a dipole which is opposite to that due to the sulfur atom [see Fig. 4(c) where we report the electrostatic potential for different coverages]. The substituent-induced dipole is poorly described (underestimated) at the PBE level (as well as at the PBE0) and a total dipole *opposite* in sign to the reference CC2 results is obtained. A rather balanced description is found with the BHLYP (Ref. 34) functional (including 50% of HF exchange), which gives a moderately strong dipole on the CF_3 group [see Fig. 4(d)] and thus a total dipole in reasonable agreement with the CC2 value and a correct description of the work functions shift. At higher coverages, the SPICE approach at the CC2 and BHLYP level predicts an unexpected work-function shift evolution with the coverage (initially increasing in absolute value and finally decreasing) due to the interaction of opposing dipoles. This effect is not captured by the PBE functional and cannot be described with Eq. (1).

In conclusion, the SPICE method allows an efficient and accurate evaluation of depolarization effects in SAM with any quantum-chemical approach. Thus, the limitations of conventional DFT can be avoided and also computational difficult cases can be appropriately treated. Applications to system with hundreds of atoms in the unit cell can be easily made.

We thank Turbomole GmbH for providing the TURBOMOLE program package. This work was funded by the ERC Starting Grant FP7 Project DEDOM, Grant Agreement No. 207441.

[1] N. J. Tao, Nat. Nanotechnol. **1**, 173 (2006).
[2] S. Braun, W. R. Salaneck, and M. Fahlman, Adv. Mater. **21**, 1450 (2009).
[3] S. G. J. Mathijssen *et al.*, Adv. Mater. **20**, 2703 (2008).
[4] M. L. Sushko and A. L. Shluger, Adv. Mater. **21**, 1111 (2009).
[5] A. Natan, Y. Zidon, Y. Shapira, and L. Kronik, Phys. Rev. B **73**, 193310 (2006).
[6] P. C. Rusu and G. Brocks, J. Phys. Chem. B **110**, 22628 (2006).
[7] G. Heimel *et al.*, Nano Lett. **7**, 932 (2007).
[8] S. Yanagisawa, K. Lee, and Y. Morikawa, J. Chem. Phys. **128**, 244704 (2008).
[9] J. Topping, Proc. R. Soc. London, Ser. A **114**, 67 (1927).
[10] B. L. Maschhoff and J. P. Cowin, J. Chem. Phys. **101**, 8138 (1994).
[11] D. Cornil *et al.*, Adv. Funct. Mater. **17**, 1143 (2007).
[12] E. V. Tsiper and Z. G. Soos, Phys. Rev. B **64**, 195124 (2001).
[13] L. Bengtsson, Phys. Rev. B **59**, 12301 (1999).
[14] B. Champagne *et al.*, J. Phys. Chem. A **104**, 4755 (2000).
[15] S. Kümmel, L. Kronik, and J. P. Perdew, Phys. Rev. Lett. **93**, 213002 (2004).
[16] A. D. Becke, J. Chem. Phys. **98**, 5648 (1993).
[17] S. Kümmel and L. Kronik, Rev. Mod. Phys. **80**, 3 (2008).
[18] C. Pisani *et al.*, J. Chem. Phys. **122**, 094113 (2005).
[19] X. Wu, A. Selloni, and R. Car, Phys. Rev. B **79**, 085102 (2009).
[20] O. S. Jenkins and K. L. C. Hunt, J. Mol. Struct.: THEOCHEM **633**, 145 (2003).
[21] R. Ahlrichs *et al.*, TURBOMOLE Ver. 5.10 (www.turbomole.com).
[22] A. M. Burow *et al.*, J. Chem. Phys. **130**, 174710 (2009).
[23] A complete SPICE-DFT run on takes 5–15 min (1 cpu).
[24] J. P. Perdew, K. Burke, and M. Ernzerhof, Phys. Rev. Lett. **77**, 3865 (1996).
[25] C. Adamo and V. Barone, J. Chem. Phys. **110**, 6158 (1999).
[26] F. Della Sala and A. Görling, J. Chem. Phys. **115**, 5718 (2001).
[27] C. Lee, W. Yang, and R. G. Parr, Phys. Rev. B **37**, 785 (1988).
[28] O. Christiansen, H. Koch, and P. Jørgensen, Chem. Phys. Lett. **243**, 409 (1995).
[29] C. Hättig and F. Weigend, J. Chem. Phys. **113**, 5154 (2000).
[30] A. Schäfer, C. Huber, and R. Ahlrichs, J. Chem. Phys. **100**, 5829 (1994).
[31] L. Romaner *et al.*, Adv. Funct. Mater. **18**, 3999 (2008).
[32] S. Baroni *et al.*, PWSCF Ver. 3.2 (www.quantum-espresso.org).
[33] L. Romaner, G. Heimel, and E. Zojer, Phys. Rev. B **77**, 045113 (2008).
[34] A. D. Becke, J. Chem. Phys. **98**, 1372 (1993).